

**TH-PM-1S** THE ROLE OF DNA STRUCTURE IN THE REPLICATION PROCESS, M.L. Gefter, Department of Biology, Massachusetts Institute of Technology, 77 Massachusetts Avenue, Cambridge, Massachusetts 02142.

The enzymatic synthesis of complementary DNA proceeds regardless of the primary sequence of that DNA. Regulation of the overall process occurs at the level of initiation, rate of synthesis and termination.

Initiation of DNA chains may occur via RNA priming (Geider, K. and Kornberg, A., 1974, J. Biol. Chem. 249, 3999-4005) or by a more complex process involving the dnaG protein (Ray, R., Capon, D. and Gefter, M., 1976, Biochem. Biophys. Res. Comm. 70, 506-512).

Elongation of DNA chains requires the action of at least two proteins other than DNA polymerase to insure that the process proceeds at replication speeds. The elongation process catalyzed by DNA polymerase in the absence of other factors proceeds in a distributive manner and in the presence of other factors in a processive manner. The processive mode of synthesis insures that once the overall process of DNA replication is initiated it proceeds to completion.

The data supporting these conclusions will be discussed.

**TH-PM-2S** RIBOSOME FUNCTIONS IN PROTEIN SYNTHESIS. C.G. KURLAND, Department of Molecular Biology, Uppsala University, Uppsala, Sweden.

A variety of chemical crosslinking methods have been used to identify the functional domains of the bacterial ribosome. The smaller (30S) ribosomal subunit has a well defined surface for the binding of messenger RNA and initiation factors which has been identified by these methods. Similarly, the larger (50S) subunit has an identifiable surface for the binding of aminoacyl-tRNA and elongation factors. When these working surfaces are positioned in the 70S ribosome (30S-50S couple), it is observed that they are on opposing surfaces near to the contacting domains that stabilize the 30S-50S interaction.

These observations imply that the subunits must move during the course of protein synthesis. A specific example of subunit rearrangements controlled by initiation factor 3 has been analyzed. This factor appears to function as a switching element: it favors an interaction between messenger RNA and the 16S RNA of the 30S subunit, and blocks a putative interaction between the 16S RNA and the 23S RNA of the 50S subunit. Such a model accounts for the requirement that IF 3 be only transiently associated with the ribosome at the initiation phase of protein synthesis.

**TH-PM-3S** WINDING AND UNWINDING OF THE DNA DOUBLE HELIX. J.C. Wang, Chemistry Department, University of California, Berkeley, California 94720

Because of the double-helical structure of DNA, many processes of gene duplication and expression involve the winding or unwinding of the DNA strands. Several general aspects will be discussed. These include the fluctuations of the helical conformation under physiological conditions at which the double-stranded structure is the stable form, the unwinding of the double helix during transcription, the coupling between tertiary coiling of a covalently closed circular double-stranded DNA and processes involving winding or unwinding of the double helix, topological and kinetic aspects of strand separation, and proteins and enzymes which are involved in the winding or unwinding of the double helix.

**TH-PM-A1 STIFFNESS AND SARCOMERE CHANGES DURING A TWITCH IN FROG SEMITENDINOSUS MUSCLE BUNDLES.** J. B. Wells, M. Schoenberg, National Institutes of Health, Bethesda, MD 20014.

We have reported (Schoenberg, Wells & Podolsky, *J. Gen. Physiol.* 64:623 (1974)) a technique for measuring the stiffness of muscle by recording the transmission time for longitudinal propagation of a mechanical disturbance. Because this technique minimizes distortion of the muscle stiffness measurement caused by tendon compliance, we used it to follow the relationship of stiffness to force during a twitch. We find that although stiffness and force start to increase at about the same time, stiffness develops more rapidly. At the peak of the twitch (26°C), stiffness,  $S$ , has reached 50% of its tetanic value,  $S_t$ , whereas force,  $P$ , has reached only 25% of its tetanic value,  $P_t$ . At 6°C,  $S/S_t = 0.85$ ,  $P/P_t = 0.7$ . In order to assess how the development of force is influenced by sarcomere movements within the muscle, we developed a laser light position sensing device (resolution  $< 10 \text{ \AA}/1/2$ -sarcomere; frequency response  $> 1 \text{ kHz}$ ) for electronically recording changes in striation spacing along the muscle. Although the ends of the preparation are fixed, the preparation is not truly isometric. Preliminary results show that the preparation does not behave uniformly along its length. Some regions (sample size 0.8 mm) start to show an increasing average sarcomere length just before the peak of the twitch, while others continue to shorten well past the peak. The average sarcomere shortening following stimulation is on the order of 2% rest length for a force change from 0 to  $P_t$ ; this in and of itself results in a lag in the development of force, the magnitude of which may be estimated. Our results are compatible with the hypothesis that 1) there is not full activation (as measured by stiffness) during a twitch, either at 6° or 26°C; 2) in this preparation most of the lag between force and stiffness following stimulation is accounted for by sarcomere shortening; 3) the rising phase of the twitch is terminated because certain regions of the muscle have started to relax.

**TH-PM-A2 CROSS BRIDGE NUMBER AND THE X-RAY DIFFRACTION PATTERN OF MUSCLE.** J. E. Hartt, L. C. Yu\*, and R. J. Podolsky, Laboratory of Physical Biology, NIAMDD, NIH, Bethesda, MD 20014

The relation between isometric force and the intensities of the equatorial reflections in the X-ray diffraction pattern of frog sartorius muscle was examined. Diffraction patterns were obtained from muscles developing full isometric force (obtained by electrical stimulation) or a fraction of full force (obtained by caffeine activation). Caffeine activation was carried out by diffusing 1-2 mM caffeine into the muscle at 20°C and then causing force to develop by lowering the temperature quickly to about 5°C. The relative force was taken as the ratio of the force produced by caffeine and that obtained by electrical stimulation. We found that at low relative force the ratio of the intensities of the 11 and 10 equatorial reflections,  $I_{11}/I_{10}$ , was close to that obtained from the muscle at rest.  $I_{11}$  increased and  $I_{10}$  decreased when the force was increased; the intensity ratio appeared to increase with the force. Since isometric force is proportional to cross-bridge number (Gordon, Huxley & Julian, *J. Physiol.* 184:170 (1966)), our results indicate that the intensity ratio is a measure of cross-bridge number during isometric contraction. In addition, they provide evidence that the myosin projections remain close to the resting position until, due to the action of calcium, sites on the actin-containing filament become available for cross-bridge formation. In shortening muscle some of the cross-bridges are in different configurations than those present in isometrically contracting muscle. Since the intensities of the equatorial reflections depend on the configuration as well as the number of cross bridges (R. W. Lyman, in press), the present results leave open the question of whether the intensity ratio is also a measure of cross-bridge number in shortening muscle.

**TH-PM-A3 X-RAY DIFFRACTION PATTERNS FROM Ca-ACTIVATED SKINNED MUSCLE FIBERS.** R. W. Lyman, L. C. Yu\*, and R. J. Podolsky, Laboratory of Physical Biology, NIAMDD, NIH, Bethesda, MD 20014

It is possible to observe equatorial X-ray reflections from calcium activated muscle fibers that have been chemically skinned. Small ( $\sim 100 \text{ \mu m}$  in diameter) bundles of rabbit psoas muscle are treated briefly with 10% glycerol - 90% relaxing solution (v/v), then mounted in a standard relaxing medium (0.14 M KCl, 10 mM imidazole, 1 mM  $\text{MgCl}_2$ , 3 mM EGTA, pH 7.0). The calcium concentration (pCa) is then varied by changing the bathing solution. The equatorial diffraction pattern and developed force are both monitored. At 1°C, pH 7.0, the intensity ratio of the first two equatorial reflections,  $I_{11}/I_{10}$ , increases when the fiber bundle (sarcomere  $\approx 2.2 \text{ \mu m}$ ) is transferred from relaxing solution to an activating solution at pCa = 4.5. When returned to relaxing solution, the ratio  $I_{11}/I_{10}$  returns to its previous value. Preliminary experiments indicate that the value  $I_{11}/I_{10}$  at pCa 4.5 is about 25% higher than at pCa 9.

**TH-PM-A4 LIGHT SCATTERING DEPENDENCE UPON CROSS-BRIDGE ATTACHMENT IN SKINNED MUSCLE FIBERS.** G. M. Katz and J. P. Reuben\*, H. Houston Merritt Clinical Research Center, Dept. Neurology, Columbia University, New York, N. Y. 10032.

Scatter of incident light (475 nm) by chemically skinned muscle fibers (rabbit psoas, human quadriceps) monitored at 90° increases 100-300% when relaxed fibers at rest length ( $L_0$ ) are put into rigor (0 MgATP). The change is fully reversible on relaxation (reintroduction of MgATP). Stretch of the relaxed fiber changes the scatter signal minimally, but when the stretched fiber is again put into rigor the change in scatter signal ( $\Delta I_s$ ) is diminished.  $\Delta I_s$  approaches zero at  $L = 1.7 L_0$  when the thick-thin filament overlap is eliminated. We conclude that  $\Delta I_s$  is a function of rigor cross-bridge position or attachment to actin. The population of rigor cross-bridges can be decreased by increasing MgATP. Tension increases as MgATP is varied from 0-10  $\mu$ M and then decreases at higher concentrations (10-100  $\mu$ M); however,  $\Delta I_s$  decreases continuously. Furthermore, N-ethylmaleimide (1.0 mM) which prevents dissociation of actomyosin by MgATP also nullifies the decrease in  $\Delta I_s$ . This is additional evidence that  $\Delta I_s$  is predominantly an indicator of position or attachment of rigor cross-bridges to actin. However, the observed increase in scatter during Ca- and caffeine-tensions suggests to us that  $\Delta I_s$  may also monitor cycling cross-bridges. Supported in part by MDAA and N.I.H.

**TH-PM-A5 THE FLUCTUATIONS IN TENSION DURING STEADY STATE CONTRACTION OF SINGLE SKINNED GLYCERINATED FIBERS.** J. Borejdo\* and A. Schweitzer\* (Introduced by J. Duke) C.V.R.I., University of California, San Francisco, CA 94143.

Although it is generally believed that cyclic, alternating interactions of myosin cross bridges with ATP and actin generate mechanical impulses superimposed to produce tension, T, no direct confirmation of this hypothesis exists. We are developing an approach designed to achieve this goal. The mean square fluctuation in stationary T is inversely proportional to N, the number of active cross bridges, so for small enough N force fluctuations should be detectable by a sufficiently sensitive force transducer. We have searched for these fluctuations using a digital transducer described here. To reduce N, all but 10<sup>4</sup>-10<sup>5</sup> myosin S-1's of a single skinned glycerinated fiber were inactivated with N-ethylmaleimide. The fiber was mounted in a chamber fitting on a stage of the light microscope. The battery operated light source illuminated an opaque flag attached to a compliant rod pulled by the fiber during contraction. The deflection of the rod was proportional to muscle tension. The rectangular slit was inserted in the back focal plane of the objective to delimit a small (2 $\mu$  x 2 $\mu$ ) area which was progressively obscured by the image of the flag as it moved in response to fiber activity. The transmitted light was proportional to the deflection of the flag and hence to T. The image of the slit was expanded by a high magnification objective and the light collected by a photomultiplier tube. The resulting photo counts were fed through a pulse shaping circuit to an on-line computer which calculates the root mean square fluctuation as well as the mean persistence time (i.e. autocorrelation function) of the fluctuation. With this configuration it is possible to detect 1 nanogram of force with the frequency response of about 100 Hz while the data collection time is only 1 min. (Research supported by HL-16683, NSF PCM 75-22698, and AHA 60-CI-08).

**TH-PM-A6 RIGOR STIFFNESS: NEM TREATMENT ELIMINATES RELAXING EFFECT OF MgATP AND MODIFIES EFFECTS OF ATP WITHOUT CHANGING MECHANICAL PROPERTIES OF RIGOR MUSCLE.** M. Orentlicher, H. Houston Merritt Muscle Center, Dept. of Neurology, Columbia University, New York, New York 10032.

Rabbit-psoas muscle was chemically skinned and stored at -20° C in glycerol/saline. Muscle fibers (2-5 mm in length) were put into a rigor condition of elastic modulus 20 Kg/cm<sup>2</sup> and low tension (0.1 Kg/cm<sup>2</sup>) by replacement of relaxing saline (140 KCl, 10 EDTA, 1 MgATP) with control rigor saline (140 KCl, 10 EDTA). Temperature was 20-25° C, pH=7.0. Rigor stiffness measured with a 5 Hz sinusoidal oscillation in length (5 $\mu$  peak-to-peak) increases monotonically with stretch. Within the time resolution of these measurements (50 ms to 100 s), both tension and stiffness instantaneously follow length changes, whether produced by a slow ramp (0.1%/s) or step. Rigor stiffness induced in the presence of 5mM ATP (95 KCl, 10 EDTA, 5 ATP) was slightly lower than that of the control rigor, and the increase of rigor stiffness with stretch above initial length was reduced. Preparations in rigor were exposed to 1mM NEM for 5-10 min. Neither the stiffness nor the effect of length change on stiffness was affected. The effect of 5 mM ATP was decreased but not changed qualitatively. However, MgATP (up to 16 mM) was unable to relax the muscle; the NEM-treated muscle gave the same stiffness response to length changes in 1 or 10 mM MgATP as in 5 mM ATP. Thus, the NEM treatment produced a drastic change in the chemical response of the cross-bridges to substrate, with negligible change in their mechanical responses. Supported in part by MDAA, N.I.H.

**TH-PM-A7 CYCLIC CONTRACTION AND RELAXATION OF SARCOMERES IN ISOLATED MYOFIBRILS**  
M. S. Mooseker\*, M. Pratt\*, D. P. Kiehart\*, and R. E. Stephens. Physiology Course, Marine Biological Lab., Woods Hole, Ma.; Dept. of Anatomy, Harvard Med. School, Boston, Ma.; Dept. of Biology, Brandeis University, Waltham, Ma.; Dept. of Biology, University of Pa. Phila., Pa.  
 (Intr. by R. Linck)

Isolated myofibrils prepared from glycerinated fibers of skeletal muscle usually contract once, and only once after addition of calcium and ATP. We have observed cyclic contractions and relaxations of sarcomeres in isolated myofibrils upon addition of solutions containing ATP and low levels of free calcium ion ( $0.4 \mu\text{M}$ – $1 \text{ nM}$ ). The myofibrils were prepared by homogenization of glycerinated fibers of rabbit psoas muscle in  $75 \text{ mM KCl}$ ,  $2 \text{ mM MgSO}_4$ ,  $1 \text{ mM DTT}$ ,  $10 \text{ mM K-phosphate buffer}$ ,  $\text{pH } 7.0$ . Similar solutions with added ATP ( $0.5 \text{ mM}$ ) and calcium buffers ( $5 \text{ mM EGTA}$ ,  $0.4 \text{ mM CaCl}_2$ ) were used as contraction media. In addition to cyclic contractions that showed little coordination between adjacent sarcomeres, we also observed wave-like propagation of contractions along the length of myofibrils. In both types of motility, the contraction and relaxation of a sarcomere occurred with a frequency of  $1\text{--}2 \text{ hertz}$ . Pulsating myofibrils were almost always attached to the slide or cover slip suggesting that the force for relaxation was provided by passive stretch. At concentrations of calcium above  $1 \mu\text{M}$  or at temperatures greater than  $27^\circ\text{C}$ , typical "one-shot" contractions were observed. The observation that waves of contraction can pass along the length of a myofibril strongly suggests the existence of a mechanical component in either the activation or relaxation of actomyosin complexes in the sarcomere. A film of this phenomenon will be shown.

**TH-PM-A8 FATIGUE IN SINGLE MUSCLE FIBERS OF THE FROG, CAUSED BY TETANIC STIMULATION AND AFFECTED BY CAFFEINE, AS RELATED TO METABOLISM.** V. Nassar-Gentina\*, J.V. Passonneau\*, and S.I. Rapoport, Laboratory of Neurophysiology, NIMH, and Laboratory of Neurochemistry, NINCDS, Bethesda, Md. 20014

Single fibers of the semitendinosus muscle of *R. pipiens* were isolated in Ringer solution at  $15^\circ\text{C}$  and were fatigued by  $150 \text{ sec}$  of externally applied tetanic stimulation at frequencies of  $20 \text{ Hz}$  and  $50 \text{ Hz}$ . Tension was measured with an RCA 5734 transducer. Stimulation at  $20 \text{ Hz}$  reduced tetanic tension to  $15\%$  of the initial value and stimulation at  $50 \text{ Hz}$  reduced tension to zero. Fiber PCr fell to  $12\%$  of the pre-tetanic concentration ( $120 \text{ nmol/mg protein}$ ) at  $20 \text{ Hz}$  and to  $65\%$  at  $50 \text{ Hz}$ , but fiber ATP remained close to normal after stimulation at both frequencies. The application of  $5 \text{ mM caffeine}$  to fibers fatigued at  $20 \text{ Hz}$  produced a maximal contracture and also reduced ATP to  $25\%$  of control concentration. The results indicate that fatigue caused by tetanic stimulation at  $20 \text{ Hz}$  can be correlated with PCr consumption; however, fatigue is not due to exhaustion of ATP stores although ATP is the direct energy source for contraction. Nor is it due to intracellular sequestration of ATP, because ATP is depleted during a caffeine contracture in fatigued fibers. The findings suggest that fatigue caused by stimulation at  $20 \text{ Hz}$  is due to failure of a step in excitation-contraction coupling and that this failure can be overcome by the release of large quantities of calcium from the sarcoplasmic reticulum, due to the action of caffeine. Fatigue caused by stimulation at  $50 \text{ Hz}$ , which is not correlated with PCr depletion, may represent failure of an early step in the excitation-contraction process.

**TH-PM-A9 CONTRACTIONS OF SKELETAL MUSCLE FOLLOWING TETANOID STIMULATION.**  
A. Sandow, and J.P. Koniarek\*. Dept. of Biology, New York University, New York, N.Y.

Massive stimulation of a frog sartorius muscle by a  $100 \text{ ms}$  duration "tetanoid" stimulus consisting of, e.g. a  $2000 \text{ Hz}$  series of  $2\text{X}$  maximal  $0.2 \text{ ms}$  shocks or a single  $1\text{X}$  maximal shock, produces a steady tetanoid response of only  $0.3 \text{ Po}$  followed by a phasic output of about  $200 \text{ ms}$  duration with additional, peak tension of  $0.35 \text{ Po}$ . The derivative ( $\dot{P}$ ) of the post-tetanoid onset includes a latent period ( $3 \text{ ms}$  at  $20^\circ\text{C}$ ), a latency relaxation (LR), and an initial rapid rise of  $\dot{P}$  to a knee, all essentially the same as in a normal twitch initiated by an action potential, except that the LR depth is only  $0.2$  of normal. Thus the post-tetanoid onset must be generated by an action potential and associated excitation-contraction coupling (ECC). Attempts to record such an action potential by an internal electrode have so far been frustrated by the very large artifacts of the tetanoid shock. But it, and a few smaller action potentials, can be detected by a special diphasic external method and their timing suggests they arise by anodal, break excitation, thus comprising a "Ritter's tetanus". But the basis of the massively generated anodal break change in polarization remains to be determined. The reduction in size of the post-tetanoid LR conflicts with D.K. Hill's LR theory since it occurs in a muscle having a  $0.3 \text{ Po}$  tension and, therefore, many more activated cross-bridges than in the resting muscle. This suggests that LR is not caused by breaking of activated cross-bridges. Supported by grants from the Muscular Dystrophy Associations.

**TH-PM-A10 SARCOMERE LENGTH-TENSION RELATIONS IN TETANICALLY STIMULATED AND CALCIUM ACTIVATED FROG SKELETAL MUSCLE FIBERS BELOW OPTIMUM LENGTH.** R. L. Moss, M. R. Sollins\* and F. J. Julian, Dept. Muscle Research, Boston Biomedical Research Institute, Boston, MA 02114.

The sarcomere length (SL) dependence of isometric, steady state tension development has been investigated in isolated single frog (*R. pipiens*) skeletal muscle fibers for  $SL \leq 2.20 \mu m$  at  $4-5^\circ C$ . The length-tension characteristic (LT) was first measured in the fibers while living and tetanically stimulated. Each fiber was subsequently glycerinated (CS) using the methods of Julian (*J. Physiol.*, 218, 117, 1971) and the LT measured in fiber segments (1-2mm long) which were activated in solutions of pCa 6.32 (Julian, 1971). This  $Ca^{2+}$  concentration resulted in tensions which were near maximal. Reproducibility of tension measurements and preservation of striation patterns were good. Maximum tension was measured for both living fibers and CS segments and SL was measured from light photomicrographs taken coincident with the tension maxima. Steady tensions for CS averaged 70% of that for living fibers. For each fiber and segment, measured tensions were scaled to the maximum tension developed in the range,  $SL = 2.0-2.2 \mu m$ . Expressed in this manner, there was good agreement between the LT data from the living and CS fibers for SL varying from 2.0 to about  $1.5 \mu m$ , and also between the combined LT data and the LT relation described by Gordon, Huxley and Julian (*J. Physiol.*, 184, 170, 1966). These results indicate that the characteristic form of the ascending limb of the LT relation of living, tetanically stimulated skeletal muscle fibers is not the result of a diminution in the level of Ca activation, at least in the SL range,  $1.5 \mu m$  to  $2.0 \mu m$ . (Supported by USPHS HL-16606, NSF GB-40978, AHA 73-699, MHA 1183, MHA 1183, MDAA, and USPHS fellowship HL-01210 to RLM.)

**TH-PM-A11 TETANIC AND TWITCH SARCOMERE LENGTH-TENSION RELATIONS IN LIVING SKELETAL MUSCLE FIBERS ABOVE OPTIMUM LENGTH.** F. J. Julian, R. L. Moss, and M. R. Sollins\*, Dept. Muscle Research, Boston Biomedical Research Institute, Boston, MA 02114.

Interest has recently been directed to the question of whether level of activation influences the form of the sarcomere length-tension relation. In these experiments, single frog skeletal muscle fibers were studied at about  $23^\circ C$  using a spot follower apparatus (Gordon, Huxley and Julian, *J. Physiol.*, 134, 143, 1966) to control the length of a fiber segment. Tetanic and twitch contractions were recorded at various sarcomere lengths (SL) ranging from about  $2.0$  to  $3.6 \mu m$ , i. e., full to no overlap. Twitches were recorded early after a tetanus (0.5-1.0 sec) at which time peak twitch force was less than 20% of the tetanic value. Twitches were also recorded 2 min. after the tetani when peak twitch force was greater than 20% of the tetanic value. Tetanic force decreased with increasing SL in a way similar to that described by Gordon, Huxley and Julian (*J. Physiol.*, 184, 170, 1966). Peak twitch force also fell nearly linearly with increasing SL in the case of the later twitches. However, in the case of the early twitches, when peak force was very small, increases in SL did not usually produce proportional decreases in twitch amplitude. In some cases small increases in twitch amplitude were seen at SL equal to about  $3.0 \mu m$ . In all cases twitch amplitude fell to near zero as SL approached  $3.6 \mu m$ . These results indicate that muscle or sarcomere length can influence level of activation in the range of SL beyond the plateau. This is not surprising since the shape of the twitch depends strongly on sarcomere length. (Supported by USPHS HL-16606, NSF GB-40978, AHA 73-699, MHA 1183, MDAA, and USPHS fellowship HL-01210 to RLM.)

**TH-PM-A12 OSMOTICALLY-INDUCED CHANGES IN THE FILAMENT LATTICE OF SKINNED STRIATED MUSCLE FIBERS.** E. W. April, M. Farrell\* and J. Schreder\*, Department of Anatomy, College of Physicians & Surgeons of Columbia University, New York City, 10032

Previous studies of single striated muscle fibers have suggested the plausibility of two equilibrium states within the thick filament lattice. Non-isovolumic shortening behavior in the skinned fiber lattice has been explained in terms of a mathematical model applicable to electrically balanced liquid crystalline systems (April & Wong, *J. Mol. Biol.* 101:107, 1976). In addition to the van der Waal's (attractive) and electrostatic (repulsive) forces, osmotic forces, acting across the permselective sarcolemma, affect the fiber volume and, hence, filament lattice spacing in intact fibers. Using controlled concentrations of PVP-10 (polyvinylpyrrolidone, approx. M.W. 10,000), an osmotic phase boundary can be established around the thick filament lattice of mechanically skinned muscle fibers. Skinned *Orconectes* fibers subjected to a series of relaxing solutions in which the osmolarities were adjusted with PVP-10 display Boyle-van't Hoff pressure-volume characteristics. This was determined by correlated light microscopic measurements of fiber diameter and low-angle X-ray diffraction measurements of interfibrillar spacing. Intact single fibers subjected to the same PVP-10 concentrations and measured by the same methods display similar behavior. The data support the concept that, in the presence of an osmotic phase boundary, the spacing between the thick filaments in striated muscle is a function of the osmotically determined volume available to the A-band lattice with the equilibrium primarily due to a balance between electrostatic and osmotic forces. (Supported by USPHS and MDAA grants)

**TH-PM-A13 OSMOTIC SHRINKAGE OF THE FILAMENT LATTICE IN FROG SEMITENDINOSUS MUSCLE.** B. M. MILLMAN, and T. J. RACEY\*, Department of Physics, University of Guelph, Guelph, Ontario

Small-angle X-ray diffraction has been used to determine the lattice spacing  $d_{10}$  in the A-band of frog semitendinosus muscle. Shrinkage of the filament lattice has been induced by increasing the osmotic pressure outside the lattice using two different preparations: (1) living muscle, in hypertonic Ringer's solutions; and (2) muscles from which the membrane had been removed by detergent, in concentrated solutions of high molecular weight dextran (LeNeveu, Rand, & Parsegian, 1976, *Nature* 259, 601). Using hypertonic solutions in living relaxed muscle,  $d_{10}$  decreased from a normal value of about 32nm (depending on the sarcomere length) to a minimum of 27nm in twice-normal Ringer's solution. In muscles where rigor had been induced by 4mM iodoacetic acid no such shrinkage was observed, probably because of membrane damage produced by the iodoacetic acid. In similar experiments using dextran to increase the osmotic pressure, skinned muscle fibres in rigor showed a decrease in  $d_{10}$  of 6 to 9 nm (depending on sarcomere length) to a minimum spacing of about 28nm. In this preparation, no shrinkage was observed in skinned muscle fibres which had been relaxed with ATP and EGTA. These latter results indicate that the large dextran molecules can penetrate between the filaments of relaxed muscle, but are unable to enter the cross-linked A-band lattice of muscles in rigor. In all cases where lattice shrinkage was observed, a minimum lattice spacing of about 27nm was found, at osmotic pressures of about 4000 torr. These experiments enable estimates to be made of effective filament dimensions and of the electrostatic repulsive forces acting between filaments in striated muscle.

(Supported by the National Research Council of Canada)

**TH-PM-A14 SEGMENT LENGTH MEASUREMENT IN PAPILLARY MUSCLE.** L.L. Huntsman, Center for Bioengineering, University of Washington, Seattle, WA. 98195

A new technique has been developed which permits the determination of segment length changes in selected regions of isolated papillary muscles. The method is based on the assumption that cardiac tissue remains isovolumic so that segment length is inversely related to cross-sectional area. A uniform alternating magnetic field (65kHz) is provided in the vicinity of the muscle. A small sense coil, a coil spring formed into a loop, made of 13 $\mu$  coated brass wire, encircles the muscle. The voltage induced in the loop is proportional to the area enclosed, i.e. the cross-sectional area of the muscle plus an offset. This offset is measured by calibration and subtracted. Over the calibration range of 0.4 - 1.5mm<sup>2</sup>, the resulting signal is linearly related to enclosed area ( $r=0.999$ ) with high accuracy (average error less than 0.5%). The segment length signal, the reciprocal of the area voltage, has a bandwidth of greater than 500 hertz and noise less than  $\pm 0.1\%$ . This performance allows high resolution measurement of segment length changes and permits feedback control of segment length. The responses of central region segments to altered loading, both slow changes such as after-loaded contractions and rapid changes such as quick stretch and release, have been investigated using this technique. Major qualitative and quantitative differences are observed between the actual segment responses and those inferred from measurements of whole muscle behavior.

Supported by NIH Grant GM16436.

**TH-PM-A15 VARIABLE CONTRACTILITY IN SKINNED CARDIAC MUSCLE.** G. McClellan\* and S. Winegrad, Dept. of Physiology, School of Medicine, University of Penna., Phila., Pa. 19174

When the concentration of MgATP is decreased to 2mM or less in the presence of  $\text{CrPO}_4$  buffering the amount of tension developed by an EGTA skinned rat ventricular strip at pCa between 9 and 5 is increased, and in 0.02mM MgATP, the force at pCa 5-6 is at least twice the maximum Ca-activated force in 5mM MgATP. In addition at low MgATP concentration the skinned fibers are more sensitive to Ca, responding to pCa which is too high to alter tension at MgATP of 5mM. Exposure to 0.02mM ATP or less and pCa of 6 or less for several minutes produces a decline in the subsequent contractile response to either elevated Ca or low MgATP. Treatment with Brij to destroy the membranes of the skinned fibers does not alter the tension-pCa relation in 5mM ATP but it increases the sensitivity to low ATP. After Brij treatment, contractility is inhibited by 1-2mM ATP in the presence of high Ca. Addition of a sarcolemmal fraction of rat ventricular homogenate to low ATP-high Ca solution prevents or diminishes the decline in contractility. Since rat ventricle functionally skinned by a soak in EGTA still retains many of its non-contractile proteins such as creatine phosphokinase and pyruvate kinase, the effects produced by changes in the composition of the medium can be due to action on enzymes regulating the contractile response as well as to direct effects on the contractile proteins. The combination of low ATP and high Ca should inhibit cAMP synthesis and stimulate its breakdown. The observed inhibitory effect on contractility of low ATP-high Ca may indicate that contractility is regulated by the net effect of two reactions, one in the membrane requiring ATP, presumably the formation of cAMP, and the second, a Ca-regulated, inhibitory reaction within the myofibril.

TH-PM-A16 EFFECT OF SARCOMERE LENGTH (SL) ON THE 3 EXPONENTIAL RATE PROCESSES OF CRAYFISH SAF MUSCLES. M. Kawai, P.W. Brandt and A. B. Eastwood\*, Depts. of Neurology and Anatomy, Columbia University, New York, New York 10032.

Small accessory flexor (SAF) muscles of the myochoordotonal organ have areas where thick and thin filaments are segregated at SL 6-10  $\mu$  (Eastwood et al, 1976). At longer SL all thin filaments form normal orbits around the thick filaments. Isometric tension induced by high K saline increases linearly from SL 6  $\mu$  to a plateau at 9-11  $\mu$  ( $P_0 = 18 \pm 3 \text{ N/cm}^2$ ) then declines at longer SL. We studied the kinetic properties of SAF muscles by oscillating the length sinusoidally (0.25-133 Hz; 100  $\text{\AA}$ /half sarcomere) and detecting the tension amplitude and phase. Three apparent rate constants can be determined which we presume relate to actin-myosin interaction during energy transduction. These are: a slow lead (phase advance) at  $2-3 \text{ sec}^{-1}$  (A), a lag at  $62 \pm 3 \text{ sec}^{-1}$  (B; oscillatory work), and a fast lead at  $380 \pm 16 \text{ sec}^{-1}$  (C, N = 23 for SEM). Nyquist plots of the data are similar in shape to those from regular crayfish muscles (Kawai & Brandt, 1975). Process (C) of the SAF muscles is not modified by change in SL, but (B) is slightly slowed at short sarcomeres. The magnitudes are approximately scaled to the tension. Slowing (B) in the low SL range may correlate with the presence of segregated bundles of thin filaments - a hypothesis which can be tested by comparison of the data to that from fibers where there is no segregation. We conclude that energy transduction processes are not altered by the degree of overlap in the high SL range (9-14  $\mu$ ), and therefore the kinetics of ATP hydrolysis are unaffected by large changes in actin-myosin spacing. Support in part by MDAA, N.I.H. and NSF(76-00441).

TH-PM-A17 THE FORCE-VELOCITY BEHAVIOR OF THE ABRM IN TONIC CONTRACTION. R.P. Schwarz, Jr. and W.H. Johnson, Dept. of Biology, Rensselaer Polytechnic Institute, Troy, N.Y. 12181

Theories for the molecular mechanism of "catch" in molluscan muscle attribute the passive tension maintenance to either actin-myosin interaction with a decreased linkage turnover rate (Single Linkage Hypothesis) or interaction between paramyosin in adjacent thick filaments (Independent Catch Hypothesis). Previous work indicates that the presence of the catch state decreases both the extent and the velocity of isotonic shortening. In these experiments, the force-velocity behavior of the anterior byssus retractor muscle (ABRM) of the mussel Mytilus edulis in tonic contraction has been determined using isotonic release at 15°C. In catch-inducing tonic contractions from the relaxed state the muscle follows the Hill force-velocity relationship. The presence of half-maximal catch tension during tonic contraction roughly doubles the Hill constant  $a/P_0$  and approximately halves the maximum shortening velocity;  $b/1_0$ , however, is unaltered by the presence of the catch state. In addition, the compliance of the series elasticity decreases by approximately 30% in the presence of the catch state. These results suggest that (1) the catch state causes alterations in the force-velocity behavior of the ABRM which suggest the presence of an "internal resistance to shortening" and (2) these alterations in the force-velocity behavior cannot be explained on the basis of a decreased linkage turnover rate according to the Huxley cross-bridge model.

**TH-PM-B1 MOLECULAR STABILITY OF Hb PHILLY.** T. Asakura, K. Adachi†, M. Sono‡ and J. Wiley‡  
Department of Pediatrics and Biochemistry, The Children's Hospital of Philadelphia, Phila., Pa. 19104 and Department of Medicine, University of Pennsylvania School of Medicine, Phila., Pa. 19104.

Hemoglobin (Hb) Philly (Tyr C1 (35)→Phe) is the first abnormal Hb with an amino acid substitution at the  $\alpha_1\beta_1$  contact to show markedly diminished heme-heme interaction and increased oxygen affinity (*J. Mol. Biol.* **104**, 185:1976). Although this Hb is classified as an unstable Hb, it was found that the oxy-form of Hb Philly is quite stable compared with other unstable hemoglobins when measured by heating and mechanical shaking methods. Although Heinz bodies (intraerythrocytic precipitation of denatured hemoglobin) were not detected in fresh erythrocytes, numerous inclusions were formed after incubation of the cells with brilliant cresyl blue (BCB). These results suggest that Hb Philly is destabilized by treatment with BCB. Since BCB is a strong oxidizing agent, we examined the molecular stability of met-Hb Philly and found that the met-form of Hb Philly was extremely unstable. This result suggests that intraerythrocytic precipitation of Hb Philly by treatment with BCB is due to oxidation of the heme iron into the unstable ferric met form. Further studies with the separated subunits showed that the abnormal  $\beta$ -chains of Hb Philly were markedly destabilized at pH 8, where normal  $\beta$ -chains were quite stable. The met-form of  $\beta$ -chains of Hb Philly was even more stable. These results suggest that the abnormal instability of met-Hb Philly is due to the conformational abnormality of the met-form of the  $\beta$ -chains. The deoxy-form of Hb Philly was also unstable indicating that Hb Philly does not change conformation upon deoxygenation. This may be the reason for lack of heme-heme interaction in Hb Philly. This work was supported by NIH-HL-18226 and NHLI-72-2962B.

**TH-PM-B2 KINETIC STUDIES OF CO BINDING TO VARIOUS MODIFIED HEMES.** M. Sono‡† J.A. McCray‡ and T. Asakura†, †Department of Pediatrics and Biochemistry, The Children's Hospital of Philadelphia, Phila., Pa. 19104 and ‡Department of Physics and Atmospheric Science, Drexel University, Phila., Pa. 19104.

In order to distinguish the effects of heme and protein, kinetic studies of CO binding have been performed for various protein-free hemes by the laser flash photolysis method at room temperature in two solvents: a mixture of ethylene glycol and 0.02N NaOH (80:20 v/v) (80% E.G.) and dimethyl sulfoxide (DMSO). In both of these solvents, CO-heme complexes were formed and exhibited distinct  $\alpha$ ,  $\beta$  and Soret peaks in their absorption spectra. In CO-saturated 80% E.G., the CO binding reactions showed simple pseudo-first order kinetics with half times at 22°C of 7, 10, 12, 21, 21 and 33  $\mu$ s for meso-, deuterio-, proto-, 2-formyl-4-vinyl-, 2-vinyl-4-formyl- and 2,4-diformylhemes. The corresponding order of decrease in CO combination rate correlates with increase in electron attractivity of heme side chains and is completely opposite to that for CO binding to these hemes in myoglobin (M.Sono, P.D.Smith, J.A.McCray, and T.Asakura (1976), *J. Biol. Chem.* **251**,1418-1426). Contrary to the results for myoglobin, the two isomeric formylhemes exhibited the same rate indicating that the difference observed in myoglobin is due to different interactions of the isomers with protein. The same relative order of CO binding to these hemes was found in DMSO as that obtained in 80% E.G. except that the rates were about 200 times slower. The reaction in DMSO was shown to be a replacement reaction of DMSO by CO since it was found that DMSO binds to heme as a ligand. The opposite order of the rate of CO binding to free heme and heme protein as a function of  $pK_3$  may be due to either differences in protein environment or be due to the fifth coordinate position of heme iron having a hydroxyl ion in free heme and a histidine in heme protein. Supported by NIH HL-18226 and NHLI-72-2962B and NSF BMS75-01623.

**TH-PM-B3 ALKALINE DISSOCIATION KINETICS OF SIX MAMMALIAN HEMOGLOBINS.** D.J. Goss and L.J. Parkhurst, University of Nebraska, Lincoln, Nebraska 68588.

The alkaline dissociation of human hemoglobin (tetramer→dimer) is consistent with a model involving four titratable salt bridges. These salt bridges are invariant in other mammalian hemoglobins, and six of these (cat, goat, dog, sheep, horse and beef) were studied in a laser light-scattering stopped-flow apparatus in order to assess the effects of variations in the amino acid sequences on the dissociation reactions. The general sigmoidal shape of the curve for the apparent dissociation constant ( $k$ ) VS pH (pH range 10.2 to 11.6) was similar to that obtained for human hemoglobin; however, the curves for the various species showed marked variation in the midpoint and range of dissociation constants. The rate constants at the lower portion of the curve ( $k_0$ ) varied from 0.25 sec<sup>-1</sup> (dog) to 0.75 sec<sup>-1</sup> (beef) among the species studied, and the rates at the high end of the curve ( $k_1$ ) varied from 4.6 sec<sup>-1</sup> (goat) to > 55 sec<sup>-1</sup> (dog). The range ( $k_1-k_0$ ) for individual species also varied (4 to > 50 sec<sup>-1</sup>), although the slope of the curve (log  $k$  VS pH) at the midpoint was essentially the same for all curves. An apparent shift in the  $pK$ 's of the salt bridges is suggested by the variation in midpoint from a low value of 10.7 to a high value of 11.1. The variation of the apparent rate constant with concentration permitted the determination of equilibrium constants in the alkaline pH range where ultracentrifuge measurements are difficult and unreliable. For the three species (dog, horse, beef) whose kinetic parameters span the overall observed range, there appear to be no substitutions in the vicinity of those residues in the  $\alpha$ -chains which are thought to form salt bridges necessary for the integrity of the tetramer (99, 127, 141) but substitutions are found near the important  $\beta$ -chain sites (1, 132, 146). Grant support: NIH 15284-05; Research Council, University of Nebraska (NIH RR-07055-10); Research Corporation.



**TH-PM-B4 SIMULTANEOUS LASER LIGHT-SCATTERING AND ABSORBANCE KINETIC STUDIES OF THE ALKALINE TETRAMER → DIMER DISSOCIATION REACTION IN HUMAN DEOXY-HEMOGLOBIN.** Duane P. Flamig and Lawrence J. Parkhurst, Department of Chemistry, University of Nebraska, Lincoln, NE 68588.

Deoxy-hemoglobin, stripped of phosphate, shows multiphasic kinetics when monitored in the stopped-flow by either  $\text{Ar}^+$  laser light-scattering or absorbance changes in the Soret region, 430nm to 450nm. The rates observed by these two methods, however, are markedly different. For Hb (7.5  $\mu\text{M}$ ) in 50 mM  $\epsilon$ -amino caproate as the final buffer (5 mM bis-tris, pH 7.0, initially), the light-scattering half-times varied from 0.95 sec to 0.40 sec for pH 10.23 to 10.85, respectively, and the absorbance half-times varied from 0.12 sec to 0.20 sec for the same pH's. The dissociation reaction (approach to equilibrium) as a function of concentration at a given pH yields two quite different time courses when monitored by light-scattering vs. absorbance. At pH 10.45 the light-scattering half-times varied from 1.15 sec to 0.75 sec for Hb concentration 2.5  $\mu\text{M}$  to 12.5  $\mu\text{M}$ , respectively, whereas the absorbance half-times varied from 0.12 sec to 0.40 sec for the same Hb concentrations. The overall light-scattering change is slower when the Hb is not stripped of phosphate and the starting buffer is potassium phosphate. The overall half-times varied from 1.05 sec to 7.0 sec for pH 10.46 to 10.89, respectively. The absorbance changes in the Soret region, which had been thought to reflect conformational changes, are faster than those reported at 245nm (half-time  $\sim$  86 sec), the latter attributed to the exposure of a tyrosine to solvent upon dissociation. Neither absorbance measurement agrees with the light-scattering results which relate directly to the dissociation process. The simultaneous light-scattering and absorbance changes associated with dissociation must therefore involve at least three different species, two conformations, and be phosphate dependent. Grant support: NIH HL 15284-05; Research Council, University of Nebraska, (NIH-RR-07055-10); Research Corporation.

**TH-PM-B5 LIGAND-BINDING KINETICS OF HUMAN HEMOGLOBIN IN MIXED SOLVENT SYSTEMS.**

Abolghassem Y. Tehrani\* and Lawrence J. Parkhurst, Department of Chemistry, University of Nebraska, Lincoln, Nebraska 68588.

Ligand-binding measurements were carried out using stopped-flow, flash, and laser photolysis on human hemoglobin in various aqueous-organic solvent systems to explore the effect of changes in surface tension, internal pressure, and dielectric constant on various rate constants. In general, rate constants pertaining to the ligand-bound conformation (R) of hemoglobin were largely unaffected by changes in solvent composition. The rate of CO binding to the deoxy (T) form, however, was very sensitive to solvent composition. In assessing these effects, the CO-binding kinetics were fit by a 4-step Adair model with the first three binding constants treated as adjustable parameters in a Fletcher-Powell minimization routine. For the seven aqueous-alcohol systems (water:methanol, ethanol, 1-propanol, 2-propanol, n-butanol, s-butanol, t-butanol), the rate constant for binding the first CO molecule ( $k_1$ ) decreased as the surface tension decreased. This is consistent with a simple picture in which expansion of the deoxy-form leads to slower rate constants for CO-binding. In other mixed solvent systems (aqueous:acetone, dioxane, ethylene glycol, glycerol) no such simple relation was found. Grant support: NIH HL 15284-05; Research Council, University of Nebraska, (NIH-RR-07055-10); Research Corporation.

**TH-PM-B6 EFFECT OF PROTONATION AND DEPROTONATION OF IMIDAZOLE ON ELECTRON DISTRIBUTION IN HEME-PROTEIN DERIVATIVES.** Mahendra K. Mallick\*, Seong Ki Mun\*, Jane C. Chang\*, and T. P. Das, Department of Physics, SUNY at Albany, Albany, NY 12222.

In recent work<sup>1</sup>, using semi-empirical procedures for obtaining the electronic wave-functions in heme derivatives and metmyoglobin, we have shown through a comparison of predicted and experimental hyperfine constants<sup>2,3</sup> for iron and nitrogen nuclei that theory can provide a successful explanation of the electronic distribution over these molecules. Encouraged by these results, we are currently investigating the influence of substitutions<sup>4</sup> in the imidazole ligands on the electron distribution on hemeprotein derivatives. The compounds we have studied so far are the neutral and positive ion bisimidazole ferric heme complexes and also nitrosylmyoglobin in which the hydrogen of the NH bond of the imidazole ligand is replaced by a methyl group. Using the predicted hyperfine fields at the nitrogen nuclei as an index substantial differences are found in distributions over the positive ion and neutral systems corresponding respectively to having both of the imidazoles protonated or one deprotonated. Thus our results support the assignment<sup>4</sup> of the different observed electron spin resonance signals in two different bisimidazole systems to the positive ion and neutral systems. In the nitrosylmyoglobin system with methyl-substituted imidazole, we find substantial hyperfine fields at both the nitrogen nucleus of the NO ligand and that on the nitrogen atom liganded to iron. This can explain the nine line ESR hyperfine pattern observed in this compound. (Supported by a grant from National Health and Lung Institute).

1 S.K. Mun et.al. Biophys. J. 16 (2 pt. 2) page 39a (1976).

2 H. L. VanCamp, C.P. Scholes and C.F. Mulks, J. Am. Chem. Soc. 98, 4096 (1976).

3 C.P. Scholes, R.A. Isaacson and G. Feher, Biochem. Biophys. Acta. 263, 448 (1972).

4 J. Peisach, Ann. N.Y. Acad. Sci. 244, 187 (1975).

**TH-PM-B7** THE EFFECT OF SELECTIVE MODIFICATION OF  $\alpha$  AND  $\beta$  CHAINS WITH DIMETHYL ADIPIIMIDATE (DMA) ON THE OXYGEN AFFINITY OF HEMOGLOBIN. R. Pennathur-Das†, T. B. Bradley††, W. Mentzer\*††, and B. H. Lubin\*†. †Bruce Lyon Memorial Research Laboratory, Children's Hospital Medical Center, Oakland, California and Cancer Research Institute, University of California, San Francisco. ††V. A. Hospital, San Francisco, California. ††Department of Pediatrics, University of California School of Medicine, San Francisco, California.

We have previously demonstrated that treatment of red cells with 5 mM DMA, pH 8.5, for 30 min. at room temperature will result in increased whole blood oxygen affinity. To further investigate this observation, we studied the effects of selective modification to  $\alpha$  and  $\beta$  hemoglobin chains on oxygen affinity and interactions with 2,3 DPG. Hemolysates were prepared by lysing cells in distilled water. Control ( $\alpha\beta$ ) and treated ( $\alpha\beta_t$ ) hemoglobin chains were separated and reconstituted to give  $\alpha\beta_c$ ,  $\alpha\beta_t$ ,  $\alpha_t\beta_c$ , and  $\alpha_t\beta_t$  hybrids according to the methods described by Waks et al.<sup>1</sup>. The oxygen binding properties of these hybrids were measured in 0.1 M HEPES buffer, pH 7.0 at 10° C. Modification of the  $\alpha$  chains ( $\alpha_t\beta_c$ ) increased the oxygen affinity to a greater extent than modification of the  $\beta$  chain ( $\alpha\beta_t$ ). In contrast, modification of  $\beta$  chains ( $\alpha\beta_t$ ) resulted in decreased interaction with 2,3 DPG as demonstrated by oxygen affinity and differential absorption spectral measurements. These studies demonstrated that the influence of DMA on whole blood oxygen affinity can be explained by intra- rather than inter- molecular reactions involving both  $\alpha$  and  $\beta$  hemoglobin chains.

Supported by grant No. HL 17357 from the National Institutes of Health, DHEW.

<sup>1</sup> Waks, M., Yip, Y. K. and Beychok, S., J. Biol. Chem. (1973) 248, 6462.

**TH-PM-B8** THE MOBILITY OF AN "IMMOBILIZED" SPIN LABEL: APPLICATIONS TO SICKLE HEMOGLOBIN. M. E. Johnson and S. S. Danyluk, Department of Medicinal Chemistry, University of Illinois at the Medical Center, Chicago, Ill. 60612 and Division of Biological and Medical Research, Argonne National Laboratory, Argonne, Ill. 60439.

Recent theoretical studies have suggested that rotational motion of macromolecules may be monitored through the EPR spectrum of a spin label which is rigidly bound to the macromolecule. Using TEMPO-maleimide labelled hemoglobin (Hb), it is shown that the linewidths of the hyperfine extrema are the most useful parameters for obtaining macromolecular rotational correlation times. The hyperfine splitting observed in the limit of an immobilized protein matrix is found to be highly temperature dependent, increasing by more than nine gauss in going from 318°K to 77°K, and exhibiting a temperature dependence of the form  $A(T) = A_0(1 - e^{-\Delta E/kT})$  where  $A_0$  is the low temperature limit. It is suggested that this strong temperature dependence is the result of a weak hydrogen bond whose stability increases with decreasing temperature. The observed linewidths and hyperfine splittings in the limit of an immobilized protein matrix also indicate that for  $T > 5^\circ\text{C}$ , the label exhibits a small, but significant degree of motional freedom within the protein matrix itself, with the degree of mobility increasing with temperature. The methods analyzed here have been used to monitor the rotational correlation time of carbon monoxide sickle hemoglobin (HbS CO) as a function of concentration, temperature, and added inositol hexaphosphate (IHP). The results indicate that in the presence of IHP, HbS CO exhibits an increased correlation time compared to that of normal adult HbA CO, with the increase in correlation time showing a surprisingly small temperature dependence.

(Supported in part by the University of Illinois Research Board and the U.S. Energy Research and Development Administration.)

**TH-PM-B9** HYSTERESIS-LIKE BEHAVIOR OF OXYGEN EQUILIBRIUM CURVE OF S-rbc DETERMINED BY A NEW METHOD. H. Mizukami, G.A. Beaudoin†, D. Bartnicki† and E.R. Adams†, Division of Regulatory Biology Biophysics, Department of Biology, Wayne State University, Detroit, MI 48202

An instrument to determine the oxygen association-dissociation equilibrium of whole blood has been developed. Only one drop of blood sample is required to trace automatically the oxygen-red blood cell equilibrium curve in the direction of deoxygenation and reoxygenation within a total of less than 10 minutes. The whole blood is suspended in the form of thin liquid film reinforced by a micromesh. The partial pressure of oxygen is changed continuously with a gas mixing pump while simultaneously being recorded by polarographic oxygen electrodes. The spectral change of red blood cells is recorded by a dual beam spectrophotometer.

Using this instrument it is shown that the oxygen equilibrium curve of sickle cells obtained during deoxygenation is shifted to higher oxygen affinity as compared to that obtained during reoxygenation. This hysteresis-like behavior of equilibrium curves is also reflected in the Hill constant,  $n$ , being greater for deoxygenation than for reoxygenation. On the other hand, if deoxygenation is completed rapidly, the sigmoidness of the reoxygenation equilibrium curve and its oxygen affinity are greater than that obtained after slow deoxygenation. The hysteresis-like behavior is the postulated consequence of intracellular polymerization of sickle hemoglobin.

**TH-PM-B10** HIGH-RESOLUTION PROTON NUCLEAR MAGNETIC RESONANCE STUDIES OF HISTIDINE TITRATION IN HUMAN HEMOGLOBINS. I. Russu and C. Ho, Department of Life Sciences, University of Pittsburgh, Pittsburgh, Pa. 15260

Proton nuclear magnetic resonance (NMR) correlation spectroscopy at 250 MHz has been used to obtain aromatic resonances of human normal adult and sickle cell hemoglobins (Hb A and Hb S, respectively) as a function of pH. By comparing these resonances with those of a mutant hemoglobin, Hb Deer Lodge ( $\beta 2 \text{ His} \rightarrow \text{Arg}$ ), we have assigned specific resonances to the C2 and C4 protons of the histidyl residues at  $\beta 2$  position. Since this residue is close to the mutation site of Hb S ( $\beta 6 \text{ Gly} \rightarrow \text{Val}$ ), it can be used as a structural probe to monitor the environment of the  $\beta 6$  valine in Hb S. The pH titration of  $\beta 2$  resonances was followed in Hb A and Hb S in both CO and deoxy forms. The titration data were analyzed by a non-linear least squares computer curve fitting procedure. The pK values of  $\beta 2$  histidyl residues in Hb A and Hb S have been determined and the electrostatic interactions on these histidyl residues have been examined. The relationship of these results to the conformation of the amino-terminal regions of Hb A and Hb S will be discussed. (This work is supported by research grants from NIH.)

**TH-PM-B11** THE KINETICS OF MYOGLOBIN AND HEMOGLOBIN AND TRANSITION STATE THEORY. Attila Szabo<sup>†</sup>, Department of Chemistry, Indiana University, Bloomington, Indiana 47401.

The kinetics of ligand binding by myoglobin and hemoglobin are qualitatively interpreted in structural terms using absolute reaction rate theory. The binding of  $\text{O}_2$  and NO is shown to be largely diffusion controlled. This, and the exothermic nature of ligand binding suggest the existence of a reactant-like transition state. Based on such considerations, we present a simple physical picture of ligand binding which provides a framework in which much of the kinetics can be understood in terms of the structures of reactants and products. Consideration will be given to the kinetic basis of cooperativity, the differences in the kinetics of  $\text{O}_2$ , NO and CO binding, the effect of organic phosphates on the rate constants, the kinetic consequences of increasing the bulkiness of ligands in a series of alkylisocyanides, the effect of oxygenation on the rates of quaternary structure change, and the differences in the on rate constants of the  $\alpha$  and  $\beta$  chains of hemoglobin.

Acknowledgement is made to the Donors of The Petroleum Research Fund, administered by the American Chemical Society for support of this research. <sup>†</sup>Alfred P. Sloan Research Fellow.

**TH-PM-B12** RESONANCE ENHANCEMENT OF METAL-LIGAND VIBRATIONS IN THE RAMAN SPECTRUM OF MET-HEMOGLOBIN. S. A. Asher, L. E. Vickery, T. M. Schuster and K. Sauer, Department of Chemistry and Laboratory of Chemical Biodynamics, University of California, Berkeley, CA. 94720 and Biological Sciences Group, University of Connecticut, Storrs, Conn. 06268.

The resonance Raman spectra of the  $\text{F}^-$ ,  $\text{OH}^-$  and  $\text{N}_3^-$  complexes of methemoglobin (MetHb) were measured with a new Raman spectrometer utilizing a pulsed, tunable dye laser. A selective enhancement of the vibrations of the sixth axial ligand against the iron occurred upon excitation within the charge transfer bands between 590-640 nm. We assign the Raman bands due to the vibrations of the sixth axial ligand in MetHb  $\text{OH}^-$  ( $497 \text{ cm}^{-1}$ ), MetHb  $\text{N}_3^-$  ( $413 \text{ cm}^{-1}$ ) and MetHb  $\text{F}^-$  (doublet at  $443$  and  $471 \text{ cm}^{-1}$ ) on the basis of (1) their selective enhancement by excitation in the charge transfer bands and (2) a  $20 \text{ cm}^{-1}$  shift in the Raman peak of MetHb  $\text{OH}^-$  to  $471 \text{ cm}^{-1}$  following isotopic substitution of  $^{18}\text{OH}^-$  for  $^{16}\text{OH}^-$ . The doublet observed in MetHb  $\text{F}^-$  is also found in metmyoglobin  $\text{F}^-$  and thus does not arise from differences between the  $\alpha$  and  $\beta$  subunits, but must reflect the existence of 2 distinct forms of the  $\text{F}^-$  complex. Inositol hexaphosphate, which alters the allosteric equilibrium between the R and T forms of Hb, has no effect on either the frequency or intensity of the Raman peaks of any of these derivatives suggesting that no movement of the iron occurs during the proposed quaternary conformational changes induced in the met form of Hb.<sup>1,2</sup> [Supported in part by the U.S. ERDA and NSF # GB36361 to K.S., and NIH # HL 17494 and NSF BM575-16093 to T.M.S.]

1) Perutz, M. F., Fersht, A. R., Simon, S. R., and Roberts, G. C. K., *Biochem.* 13, 2174 (1974).

2) Perutz, M. F., Heidner, E. J., Ladner, J. E., Beutlestone, J. G., Ho, C., and Slade, E. F. *Biochem.* 13, 2187 (1974).

**TH-PM-B13 A KINETIC MODEL OF COOPERATIVITY IN ASPARTATE TRANSCARBAMYLASE.** M. Dembo and S.I. Rubinow, Biomathematics Division, Graduate School of Medical Sciences, Cornell University, and Memorial Sloan-Kettering Cancer Center, New York, N. Y. 10021.

A relatively simple kinetic model is proposed to simultaneously account for data on the binding of carbamyl phosphate and succinate to ATCase, for the relaxation spectrum associated with this binding, and for measurements of the initial velocity of the reaction of ATCase with respect to aspartate and carbamyl phosphate. The principal assumption of the model is that ATCase consists of three identical non-interacting cooperative dimers. The values of the parameters of this model can be determined by fitting to existing experimental evidence. Various new quantitative predictions are made that can serve as additional tests of the proposed theory.

**TH-PM-B14 ENERGETICS OF THE BINDING OF SUBSTRATES AND SUBSTRATE ANALOGS TO *E. COLI* ASPARTATE TRANSCARBAMYLASE AND ITS CATALYTIC SUBUNIT.** Norma M. Allewell\* and Barry L. Knier\* (Intr. by H.W. Wyckoff). Department of Biology, Wesleyan University, Middletown, CT. 06457.

The thermodynamics of the binding of the substrate, carbamyl phosphate (CP) and the substrate analogs, succinate and N-phosphonacetyl-L-aspartate (PALA), to *E. coli* aspartate transcarbamylase and its catalytic subunit (CSU) have been compared. These measurements provide energetic criteria which may be used to evaluate and develop models of the catalytic and allosteric mechanism. Enthalpies of binding were determined by flow micro-calorimetry in 0.1 M Tris, Hepes, and Bicine at pH 8.3 and 25°C. The dependence of the observed enthalpies on the heats of ionization of the buffers indicates that, in all cases, except the binding of CP to the CSU, complex formation is accompanied by the removal of protons from the buffer. The intrinsic enthalpies of binding, corrected for this effect, are very similar for the binding of CP to the CSU and native enzyme ( $-3.50 \pm 0.15$  kcal/mole ligand), and for the binding of CP + succinate to both proteins ( $-15.04 \pm 0.2$  kcal/mole ligand). In contrast, the enthalpy of binding of PALA to the CSU is  $-11.8 \pm 0.4$  kcal/mole, while the corresponding value for the native enzyme is  $-7.6 \pm 0.2$  kcal/mole. Comparison of these values with free energies determined by difference spectroscopy (for CP + succinate) or by kinetic analysis (for PALA) indicates that binding is enthalpy-driven in all cases. However, while the binding of CP is accompanied by a relatively large decrease in entropy, the entropy change associated with the binding of either PALA or CP + succinate is much smaller.

Supported by NIH grant AM17335.

**TH-PM-B15 X-RAY SOLUTION SCATTERING CHANGES ASSOCIATED WITH THE ALLOSTERIC TRANSITION OF ASPARTATE TRANSCARBAMYLASE (ATCase).** M. F. Moody, Biology Department, Brookhaven National Laboratory, Upton, L.I., New York 11973.

Solutions of ATCase (10 - 100 mg/ml) show substantial changes in their X-ray diffraction patterns after ligation with the transition state analogue N-(phosphoacetyl)-L-aspartate ( $>1$  molecule/active site). All these changes are at spacings larger than 18-20 Å. A provisional difference pattern (from data at 100 mg/ml enzyme) shows a small peak at 23 Å, a small trough at 29 Å and a large peak at 63 Å; and a large trough around 140 Å should be revealed by measurements at smaller angles.

These differences are most likely due to structural changes (at the quaternary and gross tertiary levels) within the enzyme molecules. Ligation causes them to expand and to become more anisotropic, in agreement with the findings of earlier hydrodynamic studies (e.g. Kirschner and Schachman, *Biochemistry* 10: 1900, 1971). The X-ray solution scattering pattern can therefore be used to monitor the enzyme's quaternary structure in the presence of different concentrations of various ligands.

Research carried out at Brookhaven National Laboratory under the auspices of the U. S. Energy Research and Development Administration.

**TH-PM-C1 A NEW METHOD OF MEMBRANE RECONSTITUTION.** M. C. Goodall and G. Sachs Laboratory of Membrane Biology, University of Alabama in Birmingham, Birmingham, Alabama 35294

The method is a synthesis of known results: the Montal-Mueller technique of forming a bilayer from two monolayers and the method of monolayer formation at a hydrocarbon-aqueous interface described by Russian workers<sup>1</sup>. We confirmed the latter results using density gradient purified gastric microsomes. With a proton acceptor (DNP) in the hydrocarbon phase we observed, with a vibrating plate electrometer, the appearance of positive charge at the interface, on addition of a redox substrate (NADH-FAD), which was discharged on the addition of ADP + Pi. With MgATP alone a positive charge was observed. These experiments showed the presence of both redox and ATP driven pumps at the interface. With essentially the same techniques as Montal-Mueller but with hydrocarbon instead of air, we were able to form bilayers with phospholipid on both sides or with microsomes (aqueous phase) on one side and phospholipid (hydrocarbon phase) on the other. The functional state of these bilayers is presently under investigation. With MgATP the conductance increases without generating a potential, suggesting a neutral  $H^+-K^+$  exchange in agreement with the results for intact microsomes<sup>2</sup>. (NIH, NSF support).

<sup>1</sup>Yaguzhinsky, L.S., Boguslavsky, L.I., Volkov, A.G., Rakmaninova, A.B. *Nature* **259**: 494-495, (1976)

<sup>2</sup>Sachs, G., Hung, H., Rabon, E., Schackmann, R., Lewin, M., Saccomani, G. *J. Biol. Chem.* in press.

**TH-PM-C2 RHODOPSIN MEDIATED PROTON FLUXES IN LIPID BILAYERS.** J. Antanavage\*, P. Chien\*, G. Ching\*, C. Dunlap\*, and P. Mueller, Department of Molecular Biology, Eastern Pennsylvania Psychiatric Institute, Phila., Penna. 19129

Mammalian rhodopsin was incorporated into planar bilayer membranes by dissolving the protein directly in the lipid solution. Such membranes show fast, light-induced conductance increases specific for protons. Under voltage clamp, the response to a continuous light input or short flash is a transient increase of the membrane conductance with a rise time of 5 msec and an exponential decay lasting from one to several seconds dependent on the temperature and the membrane lipid composition. The conductance change increases with the light intensity, the concentration of hydrogen ions in the aqueous phase and is independent of the presence of other ions including calcium. The current amplitude depends on the driving force for protons, i.e., either the applied potential or the proton concentration gradient. The current voltage curve in the light is linear and crosses the voltage axis at zero membrane potential and zero current when the proton concentration is equal on both sides of the membrane. In a proton concentration gradient the I-V curve crosses the voltage axis at the proton equilibrium potential. In the presence of ethanol the response time course is slowed and the amplitude increased in proportion to the ethanol concentration. The response amplitude is dependent on temperature with a  $Q_{10}$  of 2.4 between 20 and 40°C. From the integral of the membrane currents after a flash the number of protons crossing the membrane per absorbed photon is measured to lie between 30 and 1000 at a driving force of 100 mV. Thus, the conductance changes are of such magnitude and time course that they could conceivably function as the primary light transducer resulting in a proton-calcium exchange in the rod discs.

**TH-PM-C3 THE EFFECT OF AN UNCOUPLER ON THE LIGHT RESPONSE OF BACTERIORHODOPSIN INCORPORATED INTO A BLM BY VESICLE FUSION.** T. R. Herrmann\* and G. W. Rayfield\*, Physics Department, University of Oregon, Eugene, Oregon 97403

A very large increase is observed in the short-circuit steady-state current generated by a black lipid membrane (BLM) containing bacteriorhodopsin in the presence of carbonylcyanide m-chlorophenylhydrazone (CCCP). The bacteriorhodopsin is incorporated by vesicle fusion. These experiments suggest that when membrane proteins are incorporated into a BLM by vesicle fusion the vesicle remains intact after the fusion process.

**TH-PM-C4 RECOMBINANTS OF THE PROTEOLIPID APOPROTEIN OF MYELIN WITH DIMYRISTOYL LECITHIN.** W. Curatolo, J.D. Sakura\*, D.M. Small, and G.G. Shipley, Biophysics Division, Boston University School of Medicine, Boston, Ma. 02118, and the Biological Research Laboratory, McLean Hospital, Belmont, Ma. 02178.

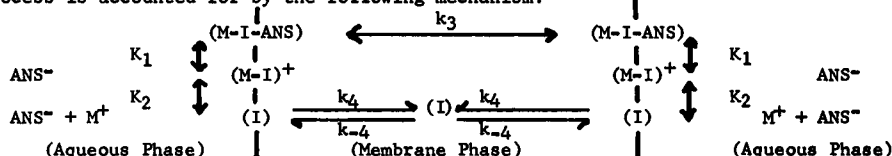
The major protein of myelin, the proteolipid apoprotein (PLA), has an unknown function. To understand how this unusually hydrophobic protein interacts with phospholipids, we have studied hydrated recombinants of bovine PLA and dimyristoyl lecithin (DML) by x-ray diffraction and differential scanning calorimetry (DSC). Both above and below the DML thermal transitions, maximally hydrated DML/PLA recombinants have a larger bilayer repeat distance than maximally hydrated DML, attributable to increased intercalation of water between the bilayers. In a DML/PLA recombinant (containing 6.3 wt. % PLA) at 37°C, a single phase is present in which the PLA molecules are homogeneously distributed throughout the DML bilayers. At 10°C, a temperature below both the DML pretransition and the order-disorder transition, two phases are present: a DML/PLA complex phase, and a small amount of unperturbed DML. DSC of DML/PLA recombinants shows the presence of a broad peak with peak maximum at approximately 2°C higher than the DML order-disorder peak. The enthalpy of this new peak increases with increasing protein content, with a concurrent decrease in the enthalpy of the sharp DML transition. This new peak represents the order-disorder transition of a population of DML molecules whose acyl chains are stabilized against melting by their association with the protein. The quantity of this "bound" lipid was estimated from calorimetry measurements to be 4 mg. DML bound/mg PLA. Model calculations indicate that this quantity of "bound" DML corresponds to 3-4 concentric layers of DML around the PLA molecule in the bilayer.

**TH-PM-C5 CATECHOLAMINE ACCUMULATION BY LIPOSOMES MAINTAINING pH GRADIENTS.** J.W. Nichols\* and D.W. Deamer, Department of Zoology, University of California, Davis CA. 95616

Liposomes, in the size range of microsomal vesicles, are formed when ether solutions of phospholipids are injected into warm aqueous solutions. The liposomes are osmotically active, most are unilamellar, and the volume trapping efficiency is approximately ten times that of sonicated and hand-shaken preparations. These liposomes were prepared with phosphatidyl choline and buffered pH gradients were established across their membranes (acidic interiors with respect to the external buffer). Such preparations efficiently concentrated several catecholamines (dopamine, norepinephrine and epinephrine) added to the external buffer in micromolar concentrations. Acetylcholine was not accumulated under similar conditions. Our observations suggest a mechanism by which pH gradients may contribute to concentration of catecholamines in sub-cellular storage sites. Supported by NSF Grant BMS 75-01133.

**TH-PM-C6 STUDY OF IONOPHORE-CATION TRANSPORT KINETICS USING 1-ANILINO-8-NAPHTHALENE-SULFONATE AS A FLUORESCENT INDICATOR.** Philip Sinkowitz\* and Duncan H. Haynes, Department of Pharmacology, University of Miami Medical School, Miami, Florida 33152

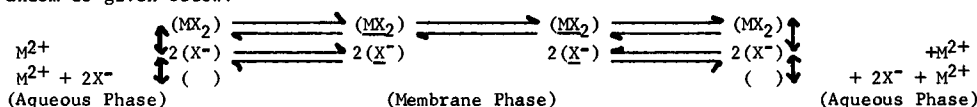
Rapid mixing of 1-anilino-8-naphthalenesulfonate (ANS<sup>-</sup>) with lecithin vesicles in a stopped-flow apparatus results in two kinetic processes: (1) an "instantaneous" fluorescent increase ( $t_{1/2}$  3 msec) attributable to binding on the outside surface and (2) a slower ( $t_{1/2}$  10 sec) representing transport to the inside surface. The slow process is speeded up by the addition of neutral ionophores (I) in the presence of monovalent cations (M<sup>+</sup>). The net process is accounted for by the following mechanism:



where  $K_1$  and  $K_2$  are the equilibrium constants of the binary and ternary complexes, respectively. The process with rate constant  $k_2$  is the rate-limiting step. For valinomycin and monactin, the  $K_1$  values show large  $\text{K}^+/\text{Na}^+$  specificities while the  $K_2$  values show large  $\text{Na}^+$  specificities. A simple explanation for this is that a poor form fit of I and M<sup>+</sup> (low  $K_1$ ) allows a closer approach of ANS<sup>-</sup> to the complexed cation (larger  $K_2$ ). The rate constant  $k_3$  shows a  $\text{K}^+/\text{Na}^+$  specificity, indicating that an optimal fit of M<sup>+</sup> and I is the most important factor determining the rate of the trans-membrane step. It is shown that the  $\text{Ca}^{2+}$  complex of X537A ( $\text{Ca-X}$ )<sup>+</sup> can behave as (I-M)<sup>+</sup> in the above scheme. (Support: NIH 1 PO1 HL 16117-01).

**TH-PM-C7 TRANSPORT KINETICS OF THE  $\text{Ca}^{2+}$  IONOPHORE X537A.** V. C. K. Chiu\* and D.H. Haynes, Department of Pharmacology, University of Miami Medical School, Miami, Florida 33152

The rate of binding and transport of X537A ( $\text{X}^-$ ) in dimyristoyl lecithin vesicles has been determined in a stopped-flow rapid mixing study of the enhancement of intrinsic fluorescence upon binding. Upon rapid mixing of  $\text{X}^-$  with vesicles, three phases of fluorescence enhancement can be observed: (1) an "instantaneous" increase ( $t_{1/2} < 2$  msec) which is attributed to binding on the outside membrane surface, (2) a fast increase ( $t_{1/2} = 15$  msec) which is attributed to insertion of the ionophore deeper into the membrane and (3) a slower process representing transport across the membrane. Processes (1) and (2) correspond to the introduction of the ionophore into the "semi-polar" and "non-polar" environments described in the previous abstract. Their  $t_{1/2}$  values are insensitive to the cation concentration whereas process (3) is accelerated by divalent ( $\text{M}^{2+}$ ) cations. For  $10^{-5}\text{M}$   $\text{X}^-$  and  $10^{-4}\text{M}$  lecithin, the acceleration obeys Michaelis-Menten kinetics for  $\text{Ca}^{2+}$  and  $\text{Mg}^{2+}$  with apparent  $K_m$  and  $V_m$  values of 0.4 mM, 6 mM and  $25 \text{ sec}^{-1}$ ,  $1.33 \text{ sec}^{-1}$ , respectively. The rates for  $\text{Ba}^{2+}$  and  $\text{Sr}^{2+}$  measured at comparable concentrations are faster, but show no tendency for saturation, implying that their  $K_m$  and  $V_m$  values are higher. At fixed  $\text{M}^{2+}$  concentration, doubling the  $\text{X}^-$  concentration doubles the rate ( $1/t_{1/2}$ ) of the process. A minimal kinetic mechanism is given below:



Additional equilibrium and kinetic information will be presented. Support: NIH P01HL16117-01.

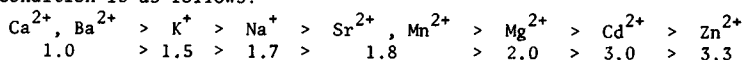
**TH-PM-C8 FLUORESCENT LIFETIME STUDIES OF THE  $\text{Ca}^{2+}$  IONOPHORE X537A IN PHOSPHOLIPID MEMBRANES** Brant Watson\* and Duncan H. Haynes, Department of Pharmacology, University of Miami Medical School, Miami, Florida 33152

Fluorescent lifetime studies were performed with the ionophore X537A and its monovalent and divalent cation complexes in organic solvents and phospholipid vesicles using the time-correlated photon counting technique. In organic solvents a single lifetime ( $\tau$ ) is seen for the anionic form of the ionophore ( $\text{X}^-$ ). The  $\tau$  value increases with decreasing solvent polarity. Binding of  $\text{X}^-$  to phospholipid vesicles results in a steady-state fluorescent amplitude characteristic of an environment of the "polarity" of methanol. Fluorescent lifetime experiments showed that the fluorophore of  $\text{X}^-$  can experience two environments which by comparison with solution data can be termed "semi-polar" ( $\tau_1$ ) and "non-polar" ( $\tau_2$ ). The time-dependent fluorescent decay ( $\text{Fl}(t)$ ) obeys the following equation when corrected for finite width of the excitation pulse:  $\text{Fl}(t) = A_1 \exp(-t/\tau_1) + A_2 \exp(-t/\tau_2)$ . The amplitudes  $A_1$  and  $A_2$  represent the number of molecules in the two states or environments and the time integral of  $\text{Fl}(t)$  is proportional to the total fluorescence observed by conventional methods. The following data below were observed for  $\text{X}^-$  complexes in dimyristoyl lecithin vesicles at  $30^\circ\text{C}$ . The data show that the increase in fluorescence observed upon complexation is due almost entirely to a shift of the  $\text{X}^-$  fluorophore from a "semi-polar" to a "non-polar" environment. These data are related to a carrier mechanism in the following abstract. Supported by Grants 1 P01 HL 16117-01 and 1F32 AM5104-01 (NIH).

Complex	$\tau_1$	$\tau_2$	$A_2/A_1$	total fluorescence
$\text{X}^-$	4.84 nsec	11.1 nsec	0.096	1.0
(K-X)	4.76 nsec	11.4 nsec	0.129	1.4
(Ca-X) <sup>+</sup>	5.19 nsec	14.0 nsec	0.129	1.4

**TH-PM-C9  $\text{Ca}^{2+}$ -IONOPHORIC PROPERTIES OF THE 20K DALTON FRAGMENT OF  $\text{Ca}^{2+}$ - $\text{Mg}^{2+}$ -ATPase IN PHOSPHATIDYLCHOLINE MEMBRANES.** Adil E. Shamoo, Department of Radiation Biology and Biophysics, University of Rochester School of Medicine & Dentistry, Rochester, N.Y. 14642.

We have shown that  $\text{Ca}^{2+}$ -dependent and selective ionophoric activity is associated with the intact  $\text{Ca}^{2+}$  +  $\text{Mg}^{2+}$ -ATPase derived from rabbit white skeletal muscle sarcoplasmic reticulum. A 20K dalton fragment obtained by controlled tryptic digestion of  $\text{Ca}^{2+}$  +  $\text{Mg}^{2+}$ -ATPase has been shown to be as  $\text{Ca}^{2+}$ -ionophore when tested in planar lipid bilayer [Shamoo, et al., JBC 251: 4147 (1976)]. The 20K dalton fragment is obtained by SDS-preparative gel electrophoresis and by SDS-column chromatography. The 20K fragment, the site of  $\text{Ca}^{2+}$ -ionophoric activity is separate from the site of ATP-hydrolysis where it has been shown to reside in a 30K fragment. Diffusion potential measurements across BLMs formed from phosphatidylcholine and cholesterol (5:1 mg/ml) in n-decane, with varying salt gradient indicate that  $P_{\text{Ca}^{2+}}:P_{\text{Cl}^-}$  varies from 2.3:1 to 5:1 depending on ionic strength. The dependency and permeability sequence as determined by at least eight experiments for each ionic condition is as follows:

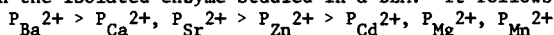


Cyanogen bromide cleavage of the 20K and subsequent isolation of the fragment with SDS-preparative gel electrophoresis, yields three fragments. Two fragments are near 4K and one is 8K. It appears that the 8K is the site of  $\text{Ca}^{2+}$ -ionophore.

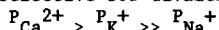
Supported by U.S. ERDA Contract and assigned Report No. UR-3490-1017. Also supported in part by NIH.

**TH-PM-C10 CHARACTERIZATION OF THE IONOPHORIC PROPERTIES OF THE 45,000 DALTON FRAGMENT OF  $\text{Ca}^{2+}$  +  $\text{Mg}^{2+}$ -ATPASE OF SARCOPLASMIC RETICULUM.** J. Abramson\*, A.E. Shamoo, (Intr. by D. A. Goldstein), University of Rochester School of Medicine & Dentistry, Rochester, N.Y. 14642.

Upon tryptic digestion of  $\text{Ca}^{2+}$  +  $\text{Mg}^{2+}$ -ATPase from skeletal muscle sarcoplasmic reticulum, the protein is cleaved into two peptide fragments: a 45K dalton fragment and a 55K dalton fragment. The 55K dalton fragment has previously been shown to act as an ionophore and also contains the site of ATP hydrolysis. The 45K dalton fragment, which is believed to be imbedded in the membrane, is separated from the other digested peptide fragments by SDS-preparative gel electrophoresis. The protein is eluted off the gel and fractions are collected. In order to remove most of the SDS, the purified 45K dalton fragment is dialyzed against 8 M Urea for 7 days followed by dialysis against water for 3 days. When studied in an artificial oxidized cholesterol black lipid membrane (BLM), the 45K dalton fragment is found to give conductance increases that are calcium dependent. The selectivity sequence is consistent with active transport of divalent cations in intact SR, and is less selective than the isolated enzyme studied in a BLM. It follows the selectivity sequence:



It is however, selective for divalent cations over monovalent cations,



Transport mediated by the 45K dalton fragment is inhibited by  $\text{HgCl}_2$  and  $\text{LaCl}_3$ , both in the 10-100  $\mu\text{M}$  range. Transport is also inhibited by incubation in mercaptoethanol or dithiothreitol. This indicates that a disulfide bond is necessary for transport.

Supported by U.S. ERDA Contract and assigned Report No. UR-3490-1018 and supported in part by NIH.

**TH-PM-C11 INTERRUPTION OF CALCIUM TRANSPORT BY DISSECTION OF THE LINKAGE BETWEEN THE HYDROLYTIC AND IONOPHORIC SITES OF SARCOPLASMIC RETICULUM  $\text{Ca}^{2+}$  +  $\text{Mg}^{2+}$ -ATPase.** Terrence L. Scott\* and Adil E. Shamoo (Intro. by J. Puskin), Dept. of Radiation Biology & Biophysics, University of Rochester School of Medicine & Dentistry, Rochester, N.Y. 14642.

Controlled digestion of sarcoplasmic reticulum vesicles with trypsin in the presence of 1 M sucrose allows a graded pattern of appearance and disappearance of four primary fragments of the  $\text{Ca}^{2+}$  +  $\text{Mg}^{2+}$ -ATPase. Assays of ATP hydrolysis and  $\text{Ca}^{2+}$  transport activities are correlated with the varying amounts of these four fragments as determined from scans of SDS-PAGE gels. At the first cleavage, in which the 100K dalton ATPase molecule is split into fragments of 55K and 45K daltons, hydrolytic and  $\text{Ca}^{2+}$  transport activities remain at the level of undigested ATPase. The hydrolytic activity is maintained at this value as the 55K dalton fragment is split. However, as the 55K fragment is cleaved  $\text{Ca}^{2+}$  transport activity declines rapidly and is correlated with the disappearance of the 55K and the appearance of the 30K and 20K peptides derived from the 55K. Thus, the two functions are uncoupled at the point of cleavage of the 55K peptide to 30K and 20K fragments, hydrolysis remaining intact while transport is abolished. Passive  $\text{Ca}^{2+}$  efflux of vesicles subjected to graded tryptic digestion indicates that increased leakage of  $\text{Ca}^{2+}$  is not responsible for transport inhibition. This dissection of the linkage between the two functions is supported by the fact that the 20K peptide has been shown to have  $\text{Ca}^{2+}$ -dependent and -selective ionophoric activity in bilayer lipid membranes, while the 30K fragment contains ATP-binding and phosphorylation site(s).

Supported by US ERDA Contract and assigned Report No. UR-3490-1024 and also supported by NIH and Muscular Dystrophy Association of America.

**TH-PM-C12 FURTHER OBSERVATIONS ON THE HYPOTHESIS OF A  $\text{K}^{+}$  SELECTIVE PHOSPHOLIPID CHANNEL IN Na-K-ATPase.** Edward S. Hyman, Touro Research Institute, New Orleans, La. 70115

Hydrolysis of the high energy acyl-phosphate (E.P) of Na-K-ATPase is dependent upon  $\text{K}^{+}$  or a slightly larger monovalent cation ( $\text{K}^{+} = \text{Rb}^{+} > \text{Tl}^{+} = \text{NH}_4^{+} > \text{Cs}^{+}$ ), but larger cations, such as hydroxylamine and its derivatives, are ineffective presumably because of limited access to the E.P site. In a study of substituted amines  $\text{HONH}_3^{+}$  and the more stable  $\text{CH}_3\text{NH}_3^{+}$  were found to be minimally effective substitutes for  $\text{K}^{+}$  in Pi formation and no other amine was effective. Larger amines,  $\text{Ca}^{++}$ ,  $\text{Ag}^{+}$ , and  $\text{Zn}^{++}$  inhibited Pi formation in the presence of  $\text{K}^{+}$ . Because the pattern of substitution and of inhibition paralleled conduction by the sphingomyelin-cardiolipin membrane, and not by shuttle-bus ionophores or by channel forming peptides, it was postulated that these phospholipids could limit access to the active E.P site (Hyman, E.S., *Biophysical J.*, 16, 28a, 1976). To associate these effects with the hydrolytic step of Pi formation, the related  $\text{K}^{+}$  dependent p-nitrophenyl phosphatase function of ATPase was studied. The effects of each cation were found to be the same as in Pi formation. Preliminary studies of ATPase using  $\text{ATP} \cdot \text{P}^{32}$  also show a similar pattern of effects on the decay of  $\text{E} \cdot \text{P}^{32}$ , but they also show other effects on partial enzyme reactions. Higher alkali amines inhibit ATP binding as well as  $\text{E} \cdot \text{P}^{32}$  decay, and there is a suggestion that they slow E.P formation after ATP binding. Unlike the corresponding alcohols, the effect of the amines is progressive and irreversible. These observations are consistent with the postulate that a  $\text{K}^{+}$  selective phospholipid channel gates cations to the E.P site.

Supported by NIH Grant AM 12718



**TH-PM-D1 ESTIMATION OF REFLECTION COEFFICIENT AND PERMEABILITY SURFACE OF PLASMA PROTEIN IN CAPILLARIES OF INTESTINE, SUBCUTANEOUS TISSUE, AND LUNG.** A.E. Taylor, D.N. Granger\*, and R.A. Brace\*, (Intr. by H.J. Granger), Dept. Physiology & Biophysics, Univ. Miss. Med. Ctr., Jackson, MS 39216

The solvent-drag reflection coefficient ( $\sigma_{p,f}$ ) and permeability surface area product ( $PS_f$ ) were estimated in several vascular beds assuming that total protein could be treated as a single solute and that the capillary membrane was homoporous. Lymph proteins were analyzed at several different volume flow states and  $\sigma_{p,f}$  and  $PS_f$  obtained by solving the solute flux equation between two different flux states. For the intestinal data,  $\sigma_{p,f}$  increased from .3 to .8 as venous pressure was elevated from 0 to 30 mm Hg (lymph flow increased 7-fold over this pressure range).  $\sigma_{p,f}$  increased from 0.82 to 0.95 as venous pressure was elevated from 5 mm Hg to 30 mm Hg in subcutaneous tissue (lymph flow increased 12-fold over this range). For lung tissue,  $\sigma_{p,f}$  was only approximated at two venous pressures and averaged 0.70 (representing a 7-fold increase in lymph flow). Our studies indicate that the capillary exchange system cannot be described by a single  $\sigma_{p,f}$  since  $\sigma_{p,f}$  is a function of volume flow across the capillary exchange membrane. If the capillary membrane could be approximated by a homoporous model, then  $\sigma_{p,f}$  would be constant and not a function of volume flow. Therefore, a simple homogenous approach will not be adequate in describing the capillary membrane and at least four parameters are necessary to describe this heteroporous membrane; the osmotic reflection coefficient, hydraulic conductance, solute permeability and the solvent drag reflection coefficient as a function of solvent flow. (Supported by HL 11770 and HL 15680)

**TH-PM-D2 EFFECT OF CAPILLARY HETEROPOROSITY ON ESTIMATES OF REFLECTION COEFFICIENT AND PERMEABILITY-SURFACE AREA PRODUCT FOR PLASMA PROTEINS.** R.A. Brace\*, A.E. Taylor, D.N. Granger\*, and A.C. Guyton, Dept. Physiology & Biophysics, University of Mississippi School of Medicine, Jackson, MS 39216

The solvent drag reflection coefficient ( $\sigma_f$ ) and permeability-surface area product ( $PS$ ) for the plasma proteins can be estimated by solving the Kedem and Katchalsky equation. Solution requires determining the lymph flow rate and lymph to plasma concentration ratio ( $R$ ) for the plasma proteins under two steady-state conditions. Implicit with this method is the assumption that the capillary membrane is homoporous. Since the capillary membrane has been shown to be heteroporous, we examined the effects of heteroporosity on estimates of  $\sigma_f$  and  $PS$  using a two pore computer model. Homoporous estimates of  $\sigma_f$  and  $PS$  significantly underestimate the true  $\sigma_f$  and  $PS$  of a heteroporous membrane. Both experimental and model data indicates that the capillary cannot be represented as a homoporous membrane when describing protein fluxes. This inability to accurately estimate  $\sigma_f$  and  $PS$  results because  $\sigma_f$  is not a constant but changes considerably with lymph flow rate. In addition, the solvent drag reflection coefficient is not generally equal to the osmotic reflection coefficient ( $\sigma_d$ ) of the Starling equation. For example, for a two pore model with  $\sigma_1=.9$  and  $\sigma_2=.5$ , depending on additional parameters,  $\sigma_d$  can equal .77 and  $\sigma_f=1.2$  while the homoporous estimate of  $\sigma_f$  is .52. It appears that the best estimate of  $\sigma_f$  and  $\sigma_d$  for a heteroporous membrane is equal to 1-R under conditions of maximal washdown of interstitial proteins. Supported by NIH grants HL 15680 and HL 11678.

**TH-PM-D3 ESTIMATION OF EQUIVALENT PORE RADIUS OF THE CAPILLARY MEMBRANE IN THE SMALL INTESTINE.** D.N. Granger\* J.P. Granger\*, and A.E. Taylor. Dept. Physiology & Biophysics, University Miss. School of Medicine, Jackson, Miss. 39216.

Systemic arterial pressure, superior mesenteric (SM) arterial pressure and flow, SM venous pressure and intestinal volume were monitored in an *in situ* cat ileum preparation with intact innervation and lymphatic drainage. After establishing an isovolumetric state, a hyperosmotic solution (1-2 molar) of either urea, glucose, mannitol, or maltose was directly infused into the SM artery at a constant rate, increasing the calculated plasma osmolality by 175-250 mOsm. The initial rate of volume loss during the infusion divided by the osmotic pressure exerted by the test solute in the SM arterial blood was used to estimate the osmotic conductance of the capillaries ( $Lo$ ). The hydraulic conductance ( $Lp$ ) was determined by the initial rate of volume increase per unit change in calculated capillary pressure. The reflection coefficient for each solute ( $\sigma_s$ ) was determined by dividing  $Lo$  by  $Lp$ . The  $\sigma_s$  values ( $\pm$  SEM) obtained for urea, glucose, mannitol and maltose were  $3.43(\pm 1.24) \times 10^{-4}$ ,  $10.1(\pm 1.47) \times 10^{-4}$ ,  $8.49(\pm 1.67) \times 10^{-4}$  and  $8.22(\pm .875) \times 10^{-4}$ , respectively. Using theoretical curves (Levitt, *Biophys. J.* 15:533, 1975) of  $(1 - \sigma_s)$  vs molecular radius of test molecule,  $\sigma_s$  of urea, glucose, mannitol, and maltose are best described by curves representing 300-500 Å radius pores. These results indicate that the classical osmotic transient approach, when applied to the small intestine, yields pore estimates which correlate to the available ultrastructural data. Supported by NIH grant HL 15680.

**TH-PM-D4 ANALYSIS OF ANTIDIURETIC ACTION THROUGH MATHEMATICAL MODELLING AND IDENTIFICATION.** G.Prevo<sup>†</sup>, J.F.Boisvieux<sup>†</sup>, P.Ripoche<sup>†</sup> and J.Bourguet. ADERSA/GERBIOS, 53 av. de l'Europe, 78140 Velizy (France) and Dept. de Biol. CEN/Saclay (France).

Analysis of the time course of net water flow through frog urinary bladder has previously led to a tentative model characterized by both a time limiting equilibrium reaction, located at the end of the sequence of events leading to the permeability variation, and a strong dependence of this equilibrium reaction upon epithelial cell volume.

We precise this model by the study of nine characteristic experimental conditions. The present model supposes the existence of two membranes in series, basal and mucosal, delimiting a cellular and two external compartments. The cellular volume and the trans epithelial net water flow are dependent upon a) external osmotic conditions b) basal permeability, which is supposed to be constant and c) mucosal permeability which is low at rest but can be increased by an activator molecule through a rapid and highly sensitive mechanism. Activator molecule is involved in a time limiting equilibrium ; its production is enhanced by ADH through cyclic AMP. Hypertonic conditions corresponding to cell shrinkage inhibit its destruction ; Hypotonic conditions, on the other hand, accelerate its inactivation, but have an additional and opposite side effect : a rapid increase in permeability which is however subsequently masked by their inactivating effect.

We show that a straightforward mathematical expression of these hypothesis, allows a satisfactory simulation of all the experiments, in conditions where all the parameters, found by optimisation methods, are both consistent and, when they correspond to known phenomena, have reasonable values.

**TH-PM-D5 THE MEMBRANE TRANSPORT MATRIX: EXPERIMENTAL EVALUATION.** A. Zelman, Center for Biomedical Engineering, Rensselaer Polytechnic Institute, Troy, NY 12181.

This report describes experimental and analytical methods of resolving frequently encountered problems of linearity, accuracy, reproducibility, reliability, and concentration polarization in characterization of membrane transport coefficients. An apparatus has been constructed for nonsteady-state characterization of membrane transport. This apparatus employs simultaneous monitoring of salt and volume transport in each half-cell, independently, to provide internal checks on accuracy. Sufficient data are generated from a single experiment to evaluate a complete matrix of coefficients ( $L_p$ ,  $\sigma$ ,  $\omega$ ). Ambiguities resulting from combining data from different experimental conditions in a single coefficient matrix are completely eliminated. Two analytical-experimental methods are employed: the zero volume flux method (ZVFM) and the linearization of the flux equations leading to the least squares straight line method (LSM). Average reproducibility of a coefficient matrix, using ZVFM or LSM, is about 5%. Average accuracies for the LSM coefficients  $L_p$ ,  $\omega$ , and  $\sigma$  are 2.9, 0.5, and 4.8%, respectively. A quantitative measure is introduced for the over-all reliability of a coefficient matrix. The "reliability coefficient,"  $R_1$ , demonstrates how well the experimental fluxes can be reproduced by the transport coefficient matrix over the range of thermodynamic forces. For these experiments  $R_{jv} \approx 3 \times 10^{-8} \text{ cm-sec}^{-1}$  and  $R_{j\omega} \approx 2 \times 10^{-10} \text{ mole-cm}^{-2}\text{-sec}^{-1}$ . The problems of linearity and concentration polarization are nearly solved, as evidenced by the reliability with which the experimental fluxes can be predicted by the transport coefficients.

Zelman, A., et al. The Membrane Transport Matrix: Analytical and Experimental Techniques for Complete Characterization, *J. Electrochem. Soc.* 123: 1015-1023 (1976).

**TH-PM-D6 THE MOVEMENT OF WATER BETWEEN BLOOD AND BRAIN.** J.D. Fenstermacher, C.S. Patlak, and H. Davson. National Cancer Institute, National Institute of Mental Health, and Fogarty International Center, National Institutes of Health, Bethesda, Md. 20014.

The exchanges of many water-soluble materials, such as Na, Cl, and urea, between blood and brain tissue are relatively slow; these reduced rates of transfer have been attributed to the tightness of the brain capillary complex, the so-called blood-brain barrier (BBB). Furthermore, the BBB restricts not only the transport of solutes between blood and brain but also the diffusional and bulk flows of water in this system. Using a computer model of water and solute transfer between blood, brain extracellular fluid (ECF), and brain intracellular fluid (ICF) and measured or assumed values for the various transfer constants,  $L_p$ ,  $P$ , and  $\sigma$ , in this system, volume and solute concentration changes in the ECF and ICF were generated for various conditions of osmotic imbalance. Over a 6 hour period, the calculated volume and solute (mainly Na and Cl) variations within the ECF and ICF compartments were small. The BBB, by restricting both water and solute exchange, seems to protect the central nervous system (CNS) from significant, short-term changes in volume which could lead to marked alterations in intracranial pressure and CNS function. In addition, pathological modifications of the BBB's transport properties as related to brain swelling (cerebral edema) will be discussed.

**TH-PM-D7 REJECTION COEFFICIENTS FOR CUPROPHANE MEMBRANE.** R. P. Wendt<sup>\*</sup>, Chemistry Department Loyola University, New Orleans, LA 70118; E.H. Bresler, Veterans Administration Hospital, New Orleans, LA 70146; E. Klein<sup>\*</sup>, Gulf South Research Institute, New Orleans, LA 70126.

In a recently published theory of heteroporous membranes,<sup>a</sup> it was shown that a simple integrated solute flux equation can serve as a good approximation to the true flux equation unless the distribution of pore sizes is bizarre (e.g., a few large pores and many small pores). The simple flux equation also fails if there is internal sieving (and consequent internal concentration polarization) within the membrane. We have applied these ideas to newly acquired data from rejection (ultrafiltration) data obtained for Cuprophane, a very wet regenerated cellulosic membrane used extensively in artificial kidney devices.

Rejection coefficients were measured for solutes of low to medium molecular weights (ca. 60-1500) and at several transmembrane volume flux densities  $J_v$ . Data were corrected for boundary layer effects using thin-film theory. Values of  $R$  vs  $J_v$  for each solute were least-squared to an integrated two-parameter rejection expression derived from the simple integrated flux equation. Values obtained for one of the parameters, the diffusive permeability coefficient, agreed well in all cases with those obtained from "pure" diffusion experiments.

The good fit of experimental data to the theoretical rejection expression indicates: (1) The pore-size distribution for Cuprophane is not bizarre in the sense previously mentioned and (2), there is no appreciable internal concentration polarization within that membrane.

<sup>a</sup> Biophys. Chem. 4:229, 237. (1976).

**TH-PM-D8 THE FACILITATED DIFFUSION OF OXYGEN BY HEMOGLOBIN AND MYOGLOBIN.** S.I. Rubinow and M. Dembo, Biomathematics Division, Graduate School of Medical Sciences, Cornell University, and Memorial Sloan-Kettering Cancer Center, New York, N. Y. 10021.

We have clarified the use of Wyman's differential equation for the facilitated oxygen flux through a slab of solution of myoglobin or hemoglobin by showing that there is a unique choice of boundary condition on the carrier concentration to be employed in conjunction with it. The singular perturbation solution of Wyman's equation, due to Murray, and Mitchell and Murray, has been extended. By means of it, the paradox of Wittenberg, that the facilitated oxygen flux per mole of heme is apparently independent of the protein carrier, has been resolved.

**TH-PM-D9 THE INHIBITION OF IODIDE TRANSPORT IN THE THYROID GLAND BY 1-ANALINO-8-NAPHTHALENESULFONATE.** G.L. Jendrasiak and T.N. Estep, Department of Physiology and Biophysics and Program in Bioengineering, University of Illinois, Urbana, IL 61801.

A model has been developed for the location of the fluorescent dye 1-analino-8-naphthalenesulfonate (ANS) at the surface of phospholipid vesicles and isolated thyroid cell plasma membranes (Jendrasiak and Estep, Chem. Phys. Lipids, in press). The presence of ANS in the bathing medium of porcine thyroid slices has a strong effect on the accumulation of iodide in the slices as given by the T/M, the ratio of iodide concentration in the slice to that present in the medium. The ANS lowers the T/M with a possible effect at concentrations as low as  $10^{-5}M$  ANS. At  $10^{-2}M$  ANS, the T/M is close to 1. The concentration of ANS necessary to attain a 50% decrease in T/M is about  $10^{-4}M$ . In the absence of ANS, the T/M value peaks at about 3 hours incubation and then slowly decreases; in the presence of ANS, the value reaches a maximum at 1 hour and remains at this value for several hours. The efflux of iodide from the gland is not affected by the ANS nor does the ANS have a measurable effect on the oxygen consumption of the slices. Inhibition of ATPase activity by ANS, as well as an increase in intracellular sodium content of thyroid cells suggest that ATPase inhibition may partially account for the lowering of the T/M by ANS; the evidence, however, is not compelling and other explanations such as the creation of a negative surface charge at the thyroid membrane interface, by the ANS, are certainly possible.

**TH-PM-D10** ALTERED PYRIMIDINE TRANSPORT IN A HUMAN MAMMARY TUMOR CELL-LINE. Peter N. Gray<sup>\*</sup>  
(Intr. by James M. Gilliam), Dept. Biochemistry and Molecular Biology, Univ. of Oklahoma  
Health Sciences Center, Oklahoma City, OK 73190.

Mammary cell carcinomas have been shown to have heterogenous properties in their responses to hormones and pyrimidine analog chemotherapeutic agents. This refractoriness to normal treatment has complicated therapeutic protocols. We have an established cell line of a human mammary ductal-cell carcinoma, BOT-2 (Nordquist, *et al.*, 1975, *Can. Res.* 35:3100) which demonstrates many of the altered properties seen *in vivo*. Although BOT-2 cells divide rapidly and grow to high population densities, we were initially unable to obtain DNA labeled with <sup>3</sup>H-thymidine in the culture medium. Since the initial observation with thymidine, we have been able to show that the defect is in thymidine transport, 0.03% of normal, (by autoradiography) and not in thymidine kinase activity, which these cells have in abundance. The transport deficiency applies to several pyrimidine nucleosides including uridine, deoxycytidine and 5-bromodeoxyuridine. No inverse alteration with promotion of base uptake was seen. These same cells are fully capable of transporting ribo- and deoxy-ribo- purines and incorporating them into acid insoluble material. Although a significant role for estrogen and androgens has been indicated in the stimulation of thymidine uptake by other mammary tumor cell lines, both estradiol and testosterone are unable to stimulate utilization by BOT-2 cells. Likewise, serum plays no role in stimulating or inhibiting thymidine uptake. The separation of thymidine transport from phosphorylation is enabling further studies on membrane function and metabolic regulation. (This research is supported by the Elsa U. Pardee Foundation).

**TH-PM-D11** THE EFFECT OF HYDRATION ON THE WATER CONTENT OF HUMAN ERYTHROCYTES R.L. Levin,  
E.G. Cravalho<sup>\*</sup> and C.E. Huggins<sup>\*</sup>, Department of Mechanical Engineering, Massachusetts  
Institute of Technology, Cambridge, Mass. 02138

An ideal, hydrated, non-dilute pseudo-binary salt-protein-water solution model of the RBC intracellular solution has been developed to describe the osmotic behavior of human erythrocytes during freezing and thawing. Because of the hydration of intracellular solutes (mostly cell proteins), our analytical results predict that at least 16.65% of the isotonic cell water content will be retained within RBCs placed in hypertonic solutions. These findings are consistent not only with the experimental measurements of the amount of isotonic cell water retained within RBCs subjected to non-isotonic extracellular solutions (20 to 32%) but also with the experimental evidence that all the water within RBCs is solvent water. By modeling the RBC intracellular solution as a hydrated salt-protein-water solution, no anomalous osmotic behavior is apparent.